

Total Dose Responses of Actel 1020B and 1280A Field Programmable Gate Arrays (FPGAs)[†]

Richard Katz
NASA/ Goddard Spaceflight Center
Greenbelt, MD, USA

Gary Swift, David Shaw
Jet Propulsion Laboratory
California Institute of Technology
Pasadena, CA, USA

Abstract

Gamma irradiation and annealing of a large number of Actel FPGAs with in-situ current measurements were performed. Lot-to-lot, part-to-part, and burn in variations were measured. Findings include a catastrophic failure mechanism and minimal dose rate effects.

I. INTRODUCTION

Designers of circuits for deployment in space are keenly aware of the advantages afforded by modern, commercial (not radiation-hardened) VLSI devices, such as memories and FPGAs: e.g., speed, density, and power consumption. Often there are a sufficient number of vendors that fortuitously radiation-tolerant devices can be found. Gate arrays are particularly attractive to designers since they can be used to replace large numbers of discrete logic devices. Field programmable gate arrays (the alternative is mask programmable) offer additional advantages in cost and schedule. As a result, a number of spacecraft incorporate Actel FPGAs. Viable alternative commercial FPGA manufacturers and technologies suitable for space applications are not yet available, but a radiation-hardened device is currently being qualified.

The silicon area in a typical FPGA is about half devoted to logic elements. The other half is used for programmable interconnects that select logic functions and route signals internally. There are two

basic types of interconnects: one-time programmable antifuses and reusable SRAM (or EEPROM)-based signal multiplexers. Commercial SRAM type FPGAs, while very popular for ground-based designs and available from several manufacturers, are difficult to use in space because they are very SEU-soft, i.e. protons and heavy ions cause SEUs that randomly redefine the circuit functionality. (Unfortunately, Harris has announced that they have abandoned an effort to provide a SEU-hardened SRAM-based FPGA.)

Actel uses an oxide-nitride-oxide (ONO) sandwich for the antifuse dielectric in their one-time programmable FPGA. Very heavy ions have been shown to cause undesired, partial connections for these antifuses, but the predicted rate of occurrence is so low that they may be usable for most space missions [1]. It remains to be seen if amorphous silicon's use as an antifuse dielectric eliminates this problem. Quicklogic has a family of FPGAs with metal-to-metal antifuses, but their single event latchup cross section is so high (greater than 10^{-3} cm² per device [2]) that it interferes with determination of reprogramming from heavy ions. The high latchup rate also makes them unattractive for space applications. A Phillips Lab-sponsored effort by Loral and Actel to build radiation-hardened versions of two Actel FPGAs is underway and includes antifuse changes intended to eliminate or reduce the chances of ion-induced connections.

The unavailability or unattractiveness of alternatives has resulted in a great deal of study of Actel FPGAs [3-6]. The present work concentrates on the total dose response of the current generation (one micron feature size) of two popular devices: the ~2000-gate A1020B and the ~6000-gate A1280A. By studying a number of samples, this study is able to

[†]The research in this paper was a cooperative effort between NASA Goddard Space Flight Center and the Jet Propulsion Laboratory, California Institute of Technology. The work at JPL was carried out under contract with the National Aeronautics and Space Administration, Code Q.

draw conclusions about lot-to-lot variations, the effect of burn-in, dose rate response differences, and bias effects. Since these are commercial devices, i.e., their radiation tolerance is not by design, some of the results are rather surprising. The results show that degradation of the internal charge pump, which applies bias to the isolation transistors, is a key factor in total dose degradation.

II. TEST METHODOLOGY

A. Test Devices.

The 1020-family of ~2000-gate FPGAs has progressed through two generations of feature sizes, the original 2.0 μ and a 1.2 μ shrink, to the current 1.0 μ feature-size devices (A1020B). While neither of the earlier devices exhibited single event latchup (SEL), the A1020B is known to have a moderate SEL susceptibility.[7] Recent heavy-ion testing also revealed clock tree upsets [2]. Thus, space applications may require circuitry for latchup mitigation and/or ways to mitigate bursts of upsets.[3] For the present study, thirty-six test samples were used. Twenty-four of the devices were burned in. They were obtained from two lots. With the exception of a single lot [5], all feature sizes of 1020-family FPGAs have been found by previous studies to be within specifications to radiation levels of at least 50 krad(Si). Some have remained functional at radiation levels above 200 krad(Si)[3-6].

Similarly, the A1280 family was originally a 1.2 μ design and is now available as a 1.0 μ shrink, the device tested for this work. Neither latchup nor clock upsets have been reported for either of the 1280 devices. Forty-eight samples from three lots (about two thirds of them were burned in) were obtained for testing. Again, with the exception of a single lot [5], previous studies have found 1280-family devices to function within specifications to levels of at least 8 krad(Si), and some over 25 krad(Si) [3-6]. It should be noted that although the feature size is the same as later 1020-family devices, the 1280-family is a later design using different design rules and incorporating numerous improvements, e.g. the charge pump is improved. The wide range of total dose results from different laboratories may be influenced by slight differences in test programs and test methodologies. However, one laboratory [5] saw a wide variation between lots

using the same test procedure, and this lot-to-lot variation is the most likely cause of reported differences in A1280 behavior. As will be seen, this study, the first with a large sample size, supports that conclusion.

B. Test Program.

Gate arrays are complex devices, and it is necessary to program them into a representative configuration in order to evaluate their radiation response. The test patterns used in this study were designed to exercise typical functions of the devices. For example, the 1280 test chip pattern was programmed into four basic sections: (1) combinatorial logic, (2) flip-flops, (3) input/output latches, and (4) shift register and counter. All functional and parametric testing was carried out on automated VLSI testers, either a Sentry S-50 or Advantest T3342. Cross checking the results from the two testers showed that they provided consistent results, and that hardware differences were not a factor in the study. The test devices were irradiated using Co^{60} at selected dose rates from 0.01 to 50 rad(Si) per second. After irradiation, some devices were subjected to several days of annealing at either room temperature or 100° C. Annealing was always done under static bias. Some tests were run with dynamic bias during irradiation, but most were statically biased.

In some cases special measurements of power supply current were made during irradiation with a strip chart recorder. Startup currents were measured between irradiations using a current probe and oscilloscope. These techniques were used to provide a more accurate determination of specific details of the device response, enhancing the parametric measurements made with the VLSI tester.

III. TEST RESULTS

Power supply current of the two gate array types behaved very differently when they were irradiated. Figures 1 and 2 show examples of increases in power supply current for a representative A1020B and A1280A under static bias. The measurements were made during irradiation. Power supply current of the A1020B increased by less than one milliamp at 56 krad(Si). Approximately one-half of the current increase recovered after a 70-hour annealing period.

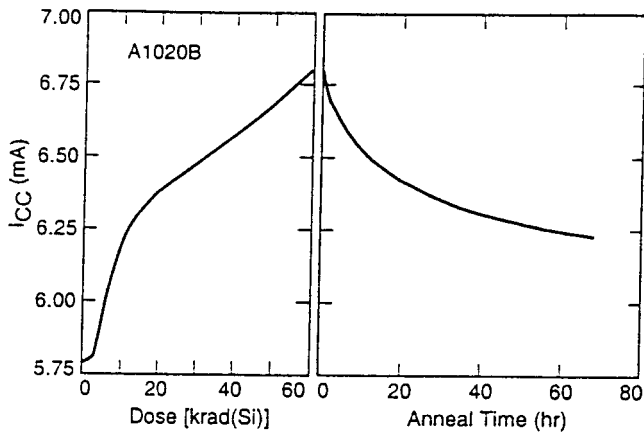


Figure 1. Increase in Power Supply Current of the A1020B During Irradiation (Static Bias).

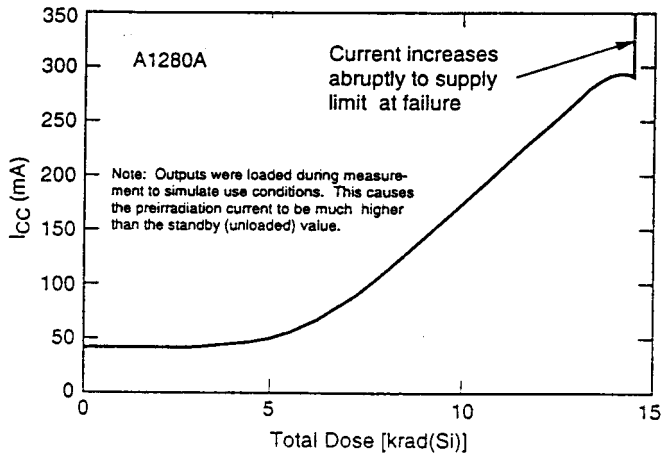


Figure 2. Increase in Power Supply Current of the A1280A During Irradiation (Static Bias)

The A1280A degraded far more severely. As shown in Figure 2, current in the A1280A begins to draw significant current well before failure, increasing in a nearly linear way until a level of about 15 krad(Si) was reached. At that point, the current jumped abruptly to a level well above the power supply current limit set point of 800 mA.. This large jump is a consistent characteristic of these experiments and has occurred as low as 12 krad(Si) for devices from other lots. Note that this is similar to the large increase in current reported in Reference 5 when irradiated parts were elevated in temperature. However, in the present study the current increases occurred at room temperature, and only the A1280A exhibited the phenomenon.

The comparison of the two device types clearly shows that one side effect of the "improvements" in the A1280A is a significantly degraded total dose

response. The design change most likely to account for this response is the two-stage bias generator used in the A1280A, which lowers the supply current for an unirradiated A1280A by more than an order of magnitude relative to the A1020B, even though there are three times as many gates in the A1280A. The total device current also depends on output loading, which is the reason that the initial current in Figure 2 is so much higher than the low standby value. The purpose of the charge pump is to ensure that the isolation FETs (needed for programming) are fully on for normal part operation. As increasing levels of total dose degrade its output capacity and increases the drive needs of the $\sim 10^4$ transistors, a significant number of the logic arrays' CMOS pairs are both on, at least partially, and thus draw significant current. Approximately one thousand logic pairs drawing current that is a significant fraction of 1 mA are enough to account for the largest currents observed (almost 1.5 amps). This is consistent with one of the proposed explanations and the accompanying SPICE model of Reference 5. Dynamic bias does not significantly increase the radiation tolerance, as discussed later in the paper.

Parameters other than supply current show less response to total dose, and usually remain within specification limits. These include input leakage, output voltage, and various propagation delays. Figure 3 is a representative example for the A1020. The propagation time of this sample actually decreases slightly during irradiation. However, it increases significantly during subsequent annealing. The increase in propagation delay seen during the high temperature anneal period is less than the specified maximum of 150 nanoseconds, but is large enough to cause problems with unintentionally marginal designs that are functional before irradiation. The increase in propagation delay is probably caused by interface traps (rebound effect), which do not anneal at these temperatures, although the charge pump in this circuit may also be a factor.

A few of the A1280A devices were irradiated without bias in order to determine the effect of bias on the radiation behavior. As shown in Figure 4, only very small increases occurred in power supply current when devices were unbiased. However, as shown later, subsequent irradiation of these parts with bias showed that they failed at even lower levels compared to devices from the same lot that were irradiated for the first time.

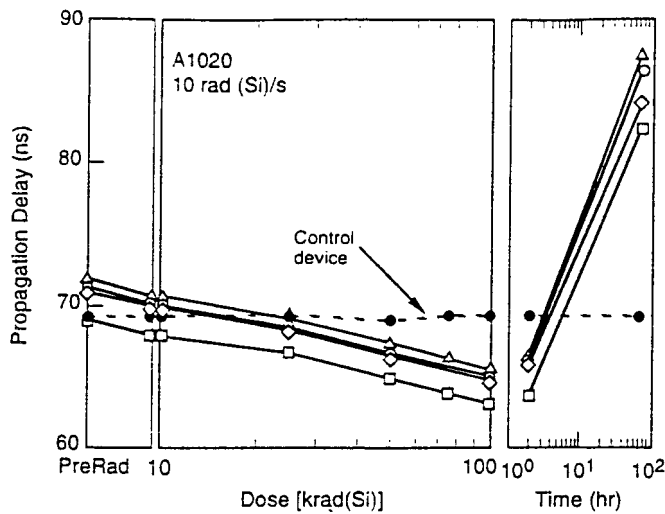


Figure 3. Degradation of Propagation Delay Time of the A1020 Showing Increase After High-Temperature Annealing.

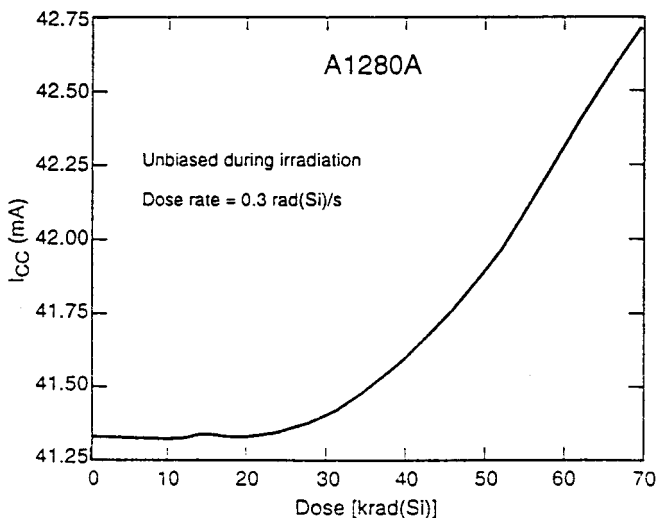


Figure 4. Effect of Total Dose on an A1280A Device Irradiated without Bias

A. Lot-To-Lot Variations

Figure 5 shows functional failure results for A1020B devices from three different lots. The y-axis represents the lowest power supply voltage at which devices were fully functional. These measurements were made while running test vectors at 5 MHz. Note that device S/N:600 from a later date code exhibited the most radiation tolerant behavior of the three, even though it is a commercial non-mil-screened device. Devices S/N's: 511 and 398 are from two different Mil-Spec lots, but began to fail functionally at much lower total doses. Response variation between burned in and non-burned in Mil-Spec parts from the

same lots was small, which may indicate that lot-to-lot variations (in the charge pump) are the likely explanation for the differences in radiation response seen here. In general devices within a specific lot exhibited very similar radiation responses, compared to parts from different lots.

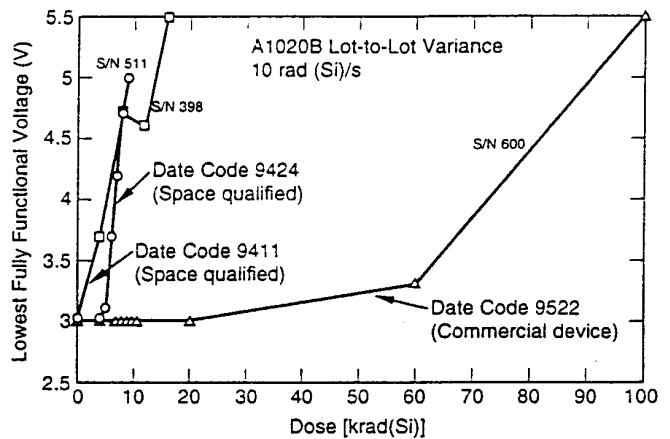


Figure 5. Comparison of A1020B Devices from Three Different Date Codes.

Additional data on the variability between lots and the effect of burn in are shown in Table 1 below. The startup current is an important parameter, which is discussed later in the paper. The key point of the table is that there are only small differences in the radiation response of parts that have not been subjected to burn in.

Table 1. Comparison of the Radiation Response of A1280A Devices with and without Burn In

Device History		Minimum Startup Current (mA)			
Lot	Burn In	Pre-rad	4 krad(Si)	6 krad(Si)	8 krad(Si)
U80	Yes	3	70	350	580
U80	Yes	3	70	360	...
U80	No	3	70	...	780
U82	Yes	3	90	320	720
U82	Yes	3	105	...	760
U82	No	3	150	350	680

B. Feature Size

Figure 6 shows supply current data ($V_{CC} = 5.0V$) for three devices with three different feature sizes. Both the 1.2 and 2 μm devices exhibited radiation tolerant behavior while the 1 μm device was well above the specification by 7 krad(Si). It increased abruptly above this level, reaching a maximum of over 250 mA at 8 krad(Si). The specification limit

for this parameter is 25 mA. The 1.2 μm FPGA was out of specification at 30 krad(Si), but did not exhibit the abrupt increases shown by the 1 μm device. All three devices were statically biased during irradiation.

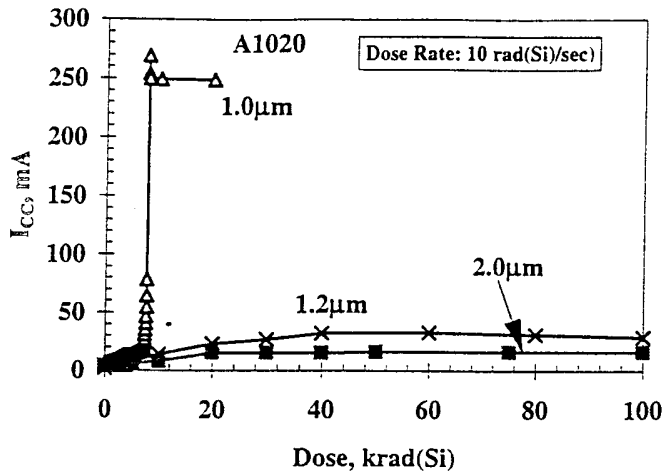


Figure 6. Comparison of the Radiation Response of A1020-Series Devices with Different Feature Size

As discussed later in this paper, the abrupt change in power supply current of the 1 μm device is caused by failure of the internal charge-pump circuitry, not field oxide inversion. The large variations in failure level between different lots are due to differences in the internal circuit margin of the charge pump. Thus, it is not possible to make a definite conclusion about the effect of feature size on total dose behavior for these devices because the differences, although large, are within the range of lot-to-lot variations of devices with the same feature size. It is unlikely that the increased sensitivity of the 1 μm device is due to device scaling, although the test results support the conclusion that an increased number of lots with smaller feature size exhibit early failure (low total dose levels).

C. Radiation Bias

The effects of bias were evaluated in several different ways. Devices were tested under static and dynamic bias conditions to determine if there were any differences, as well as without bias (see Figure 4). In addition, special measurements were made to determine the minimum power supply voltage for which devices would still function, even if the voltage was below the normal power supply range.

Figure 7 plots supply current ($V_{CC} = 5.0\text{V}$) for three A1020B devices under different bias conditions. In addition to the unbiased case, two different static biases were used: $V_{CC} = 3.3\text{V}$, $V_{OUT} = 1.65\text{V}$; and $V_{CC} = 5.0\text{V}$, $V_{OUT} = 2.75\text{V}$. As expected, unbiased devices exhibited little change after irradiation. The device biased with $V_{CC} = 3.3\text{V}$ was somewhat more susceptible to total dose, increasing to about 100 mA at 50 krad(Si). The curve showing the worst performance is for static bias with $V_{CC} = 5.0\text{V}$, $V_{OUT} = 2.75\text{V}$. Note the sharp increase in current under this bias condition above 6 krad(Si). This data shows that bias plays an important role in the radiation response of the A1020 FPGA and appears to adhere to well established understanding of CMOS radiation effects [8].

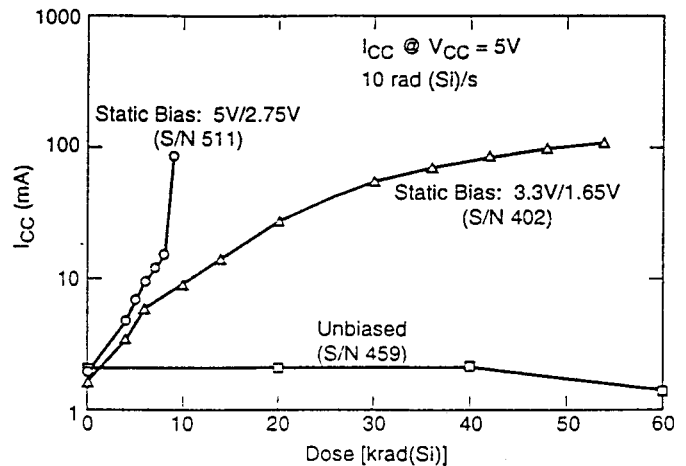


Figure 7. Effect of Static Bias Conditions on Operating Current for the Actel A1020B.

A comparison of static and dynamic bias conditions on the A1020B is shown in Figure 8. Although there are some unit-to-unit variations, these results suggest that there is little difference between static and dynamic bias for these devices.

Figure 9 compares the minimum operating voltage of two A1020B devices irradiated under worst case static and dynamic conditions at 10 rad(Si)/s. The difference in the lowest functional failure voltage is only slightly different for the two bias conditions, which agrees with the conclusion about the effect of bias on power supply current in Figure 8. This further corroborates that differences between dynamic and worst case static biases are not significant.

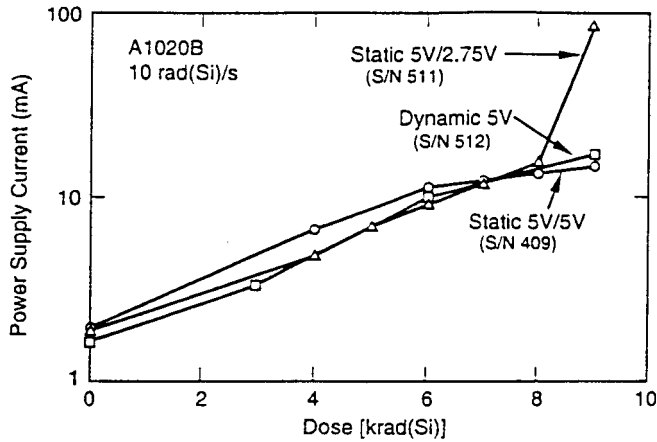


Figure 8. Dynamic vs. static bias comparison for the Actel A1020B.

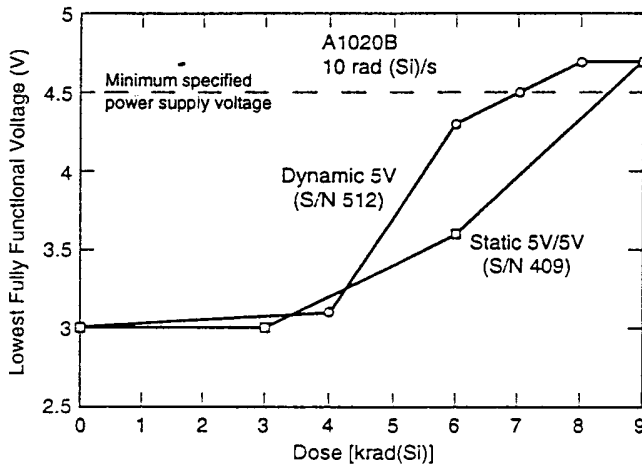


Figure 9. Minimum Operating Voltage of the 1020B Irradiated Under Static and Dynamic Operating Conditions

D. Effect of Charge Pump on Total Dose Response

A more thorough characterization of the effect of power supply voltage on operating current was used to determine the effect of total dose on minimum operating conditions. Figure 10 shows how both the operating current and the minimum operating voltage are affected by increasing levels of radiation for a statically biased device. Until a critical voltage is reached, the device does not operate normally. Before irradiation there is a slight increase in current after the minimum operating voltage is reached. As the radiation level increases, the minimum operating voltage also increases. Note that it exceeds the minimum supply voltage (4.5 V) at radiation levels between 7 and 8 krad(Si), and exceeds the maximum supply voltage at 9 krad(Si).

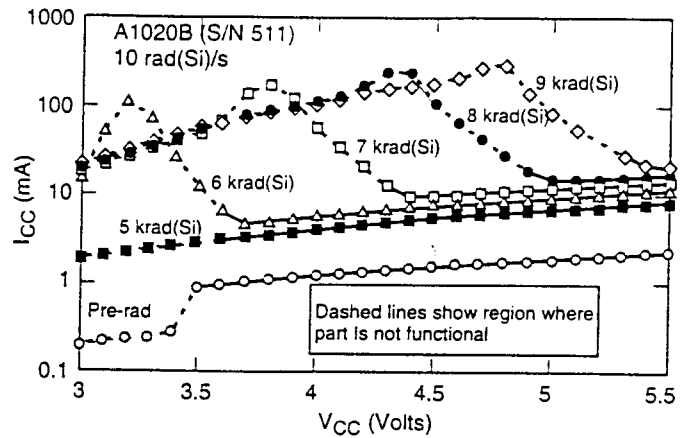


Figure 10. The Relationship between V_{CC} and Operating Current of the A1020B at Different Radiation Levels

As the charge pump degrades, there is a large increase in current at voltages below the minimum start-up voltage (these increases appear as a “bump” in the curves of Figure 10). Note that these currents can be extremely high (more than a hundred milliamps). In testing groups of devices, large variations will occur in the power supply current of different units because of the strong dependence of current on small differences in the internal margins of the charge-pump circuitry.

The A1280A also exhibits large increases in current as the charge pump degrades. It is even more sensitive to these effects because of the modified charge pump circuitry, which reduces standby current compared to the A1020-series devices. The effect of radiation on start-up current in the A1280A was shown in Table 1. The large current increases appear to be the same for devices with and without burn in.

Additional work into the effects of radiation on the charge pump was done, using the A1280A. To do this, a current probe was set up so that start-up current could be monitored as a function of time after the power was supplied to the circuit. Figure 11 plots data with this configuration. Although not shown in the figure, unirradiated devices show only a very small initial transient current (< 3 mA) after power is applied. At 4 krad(Si), the start-up transient increases to about 70 mA, as shown in the inset in Figure 11. However, this current persists for only about 1 ms. At higher radiation levels, the transient current becomes much larger, and can

extend to very long time periods. At 12 krad(Si) the circuit does not start until 35 ms has elapsed. Note that other samples have startup times as long as 150 ms at 12 krad(Si). During the time period before the charge pump becomes operational, currents of nearly one ampere flow in the device! Once the charge pump becomes operational, the current falls abruptly, but to a significantly higher level than before irradiation, as discussed earlier.

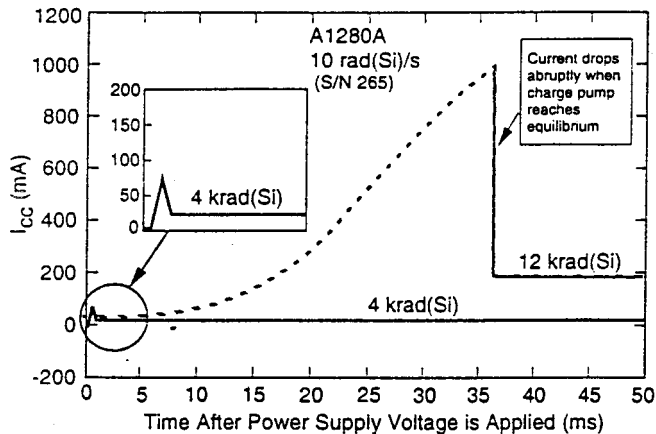


Figure 11. Start-up Current Transients in the Actel 1280A.

The large start up current brought on by radiation can become problematic for spacecraft designers. In typical spacecraft designs, the power supplies are current limited. If the device in Figure 11 (after 12 krad(Si)) is started up, it would draw a significant amount of power. Unless the power supply had a great deal of reserve capacity, then it is possible that the FPGA would not start functioning. Note that the required start-up current for the A1280A is nearly a factor of 20 higher than the pre-irradiation value of power supply current. This is a severe application problem for the Actel A1020B series of FPGA's as well as for the A1280A.

IV. DISCUSSION

The large turn-on transients of these gate arrays after irradiation are clearly a unique problem that must be considered when they are applied in specific systems. Most automated test systems (and most radiation test plans) do not evaluate turn-on conditions. The increase in current and delayed start-up time could easily be missed by a typical test system, because the normal procedure is to delay the

start of parametric and functional testing for a substantial time period after power is applied so that cable capacitances can charge. These time delays are usually not specified or carefully controlled.

However, the delayed start-up and very large transient current could easily result in failure in typical applications. If the power supply system cannot supply sufficient current, the charge pump will not start, and the device will draw large currents for extended time periods, causing severe overheating. System malfunctions may also occur if the power-on-reset delay time is not long enough to accommodate the much longer FPGA startup time of irradiated devices.

Evaluating these results leads to the following conclusions: (1) lot-to-lot variation in the degradation of both the A1020-series and A1280 gate arrays is significant, and is probably due to differences in the internal margin of the charge-pump circuits between lots; (2) part-to-part variation is also quite notable, though smaller; and (3) differences between burned in parts and those not burned do not appear to be very significant.

Since many missions conserve power by leaving systems off for a significant fraction of the time, an additional experiment was undertaken to determine how an A1280A that had been previously irradiated without bias would respond to an additional (incremental) irradiation with bias applied. The initial (unbiased) irradiation was to a level of 60 krad(Si), and the power supply current of the circuit changed very little (see Figure 7). Figure 12 shows the effect of the additional irradiation under bias. The large increase in current occurred at about one-half the radiation level of devices that were not subjected to an initial unbiased irradiation (compare with Figure 1). This shows that although parts are definitely less affected by irradiation when they are irradiated without bias, there is latent damage from the unbiased irradiations that can affect later biased irradiations.

Figure 12 also shows the annealing characteristics of the static bias current. The device anneals significantly after several hours at room temperature. While the rapid annealing was expected, the implication that unbiased irradiation causes latent damage or somehow increases the biased radiation susceptibility was not.

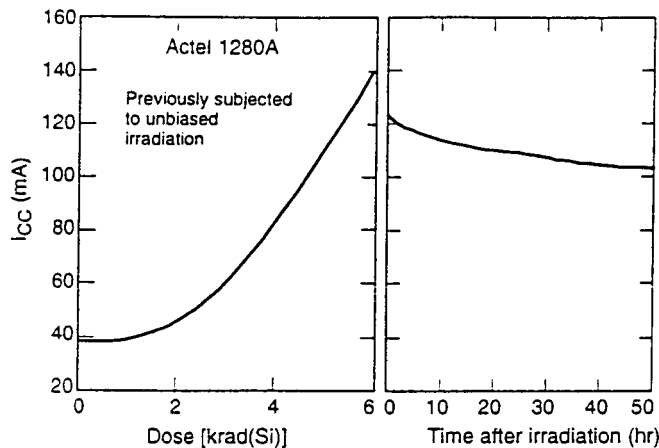


Figure 12. Effect of a Biased Irradiation on a Device Previously Irradiated without Bias

V. CONCLUSIONS

The A1020B is not nearly as tolerant to total dose as previous versions of this device with larger feature size, although substantial variations in radiation hardness occur between different production lots for all feature sizes. Total dose degradation affects the charge-pump circuit in these devices, causing large increases in the power supply current and raising the minimum operating voltage.

The improved charge pump used in the A1280 family increases its radiation susceptibility compared to the A1020-series devices. The A1280A can be expected to draw significant current (> 100 mA, static) after only a few krad(Si), well before functional failure at 10-15 krad(Si). Both device types show little part-to-part variability within a lot, but significant variations between lots. The effects of burn-in on the dose susceptibility, if any, are smaller than part-to-part variation. Irradiating an A1280A without bias significantly lowers the dose response, although it appears as if it may enhance the effects of subsequent biased irradiation. The charge pump damage of both FPGA families anneals readily. Thus, it is possible that low dose rate testing may

show a significant decrease in susceptibility for the same total dose.

The large currents that are required during start up for these devices is a significant problem for many applications. It is vitally important that radiation testing include special measurements of the start-up characteristics, which are reported for the first time in this paper. The large currents not only increase power dissipation in irradiated devices, but delay the operation of the circuit for extended time intervals after power is applied. If the power supply system cannot supply sufficient current, the charge-pump circuit will never be able to turn on, and the circuit will fail in the application at lower radiation levels.

VI. REFERENCES

- [1] G. Swift and R. Katz, "An Experimental Survey of Heavy Ion Induced Dielectric Rupture in Actel FPGAs," presented at the RADECS 95 Conference, Arcachon, France, September, 1995.
- [2] Unpublished JPL/GSFC test data taken at Berkeley 88" Cyclotron, September 21-22, 1994, and Brookhaven Single Event Test Facility, December 6-7, 1994.
- [3] R. Katz, R. Barto, P. McKerracher, B. Carkhuff, and R. Koga, "SEU Hardening of FPGAs for Space Applications and Device Characterization," *IEEE Trans. Nucl. Sci.*, **NS-41**, pp. 2179-2186, Dec. 1994.
- [4] R. Koga, W. R. Crain, K. B. Crawford, S. J. Hansel, S. D. Pinkerton, and T. K. Tsubota, "The Impact of ASIC Devices on the SEU Vulnerability of Space-borne Computers," *IEEE Trans. Nucl. Sci.*, **NS-39**, pp. 1685-1692, Dec. 1992.
- [5] Field Programmable Gate Arrays: Evaluation for Space-Flight Applications, JPL Publication 92-22, September 15, 1992
- [6] G. K. Lum, R. J. May, and L. E. Robinette, "Total Dose Hardness of FPGAs," *IEEE Trans. Nucl. Sci.*, **NS-41**, pp. 2487-2493, Dec. 1994.
- [7] R. Koga, S. J. Hansel, W. R. Crain, K. B. Crawford, and J. F. Kirshman, presentation on "Comparison of SEU and Latchup Susceptibilities of Actel's 2.0, 1.2, and 1.0 micron CMOS FPGAs," presented at the Ninth SEE Symposium, Manhattan Beach, Calif., April 19-21, 1994 (see also [1] and [6]).
- [8] T. P. Ma and P. V. Dressendorfer, "Tonizing Radiation Effects in MOS Devices and Circuits", pp. 262-269, John Wiley, NY, 1989.